axioms

MDPI

Article

The Characterization of the Mechanical Harmonic Oscillator Extremum Envelope Shape According to Different Friction Types

João C. Fernandes

Physics Department, Instituto Superior Técnicon, Av. Rovisco Pais, P-1049-001 Lisboa, Portugal; joao.ferreira.fernandes@tecnico.ulisboa.pt

Abstract

To characterize a phenomenological model of a mechanical oscillator, it is important to know the properties of the envelope of the three main physical motion variables: deviation from equilibrium, velocity, and acceleration. Experimental data show that friction forces restrict the shape of these functions. A linear, exponential, or more abrupt decay can be observed depending on the different physical systems and conditions. This paper aimed to contribute to clarifying the role that some types of friction forces play in these shapes. Three types of friction—constant sliding friction, pressure drag proportional to the square of velocity, and friction drag proportional to velocity—were considered to characterize the line connecting the maxima and minima of displacement for a generic mechanical harmonic oscillator. The ordinary differential equation (ODE), describing the harmonic oscillator simultaneously containing the three types of dissipative forces (constant, viscous, and quadratic), was numerically solved to obtain energy dissipation, and the extrema of both displacement and velocity. The differential equation ruling the behavior of the amplitude, as a function of the friction force coefficients, was obtained from energy considerations. Solving this equation, we obtained analytical functions, parametrized by the force coefficients that describe the oscillator tail. A comparison between these functions and the predicted oscillator ODE extrema was made, and the results were in agreement for all the situations tested. Information from the velocity extrema and nulls was enough to obtain a second function that rules completely the ODE solution. The correlations obtained allow for the reverse operation: from the identified extremum data, it was possible to identify univocally the three friction coefficients fitting used in the model. Motion equations were solved, and some physical properties, namely energy conservation and work of friction forces, were revisited.

Keywords: friction; harmonic oscillator; damped oscillator

MSC: 70-10

check for updates

Academic Editor: Giovanni Nastasi

Received: 16 May 2025
Revised: 17 July 2025
Accepted: 19 July 2025
Published: 23 July 2025

Citation: Fernandes, J.C. The Characterization of the Mechanical Harmonic Oscillator Extremum Envelope Shape According to Different Friction Types. *Axioms* **2025**, *14*, 554. https://doi.org/10.3390/axioms14080554

Copyright: © 2025 by the author. Licensee MDPI, Basel, Switzerland. This article is an open access article distributed under the terms and conditions of the Creative Commons Attribution (CC BY) license (https://creativecommons.org/licenses/by/4.0/).

1. Introduction

In a recent paper [1], the authors introduce a phenomenological model to describe the motion of a physical pendulum oscillator based on the product of a modulating function and a sinusoidal time phase function to characterize angular deviation: $\theta(t) = \theta_0(t)\cos(\varphi(t))$. This model can be applied to a simpler linear oscillator, provided we know the properties of the envelope of the three main physical motion variables: deviation from the equilibrium, velocity, and acceleration. Experimental data show that the friction forces completely restricted the shape of these functions: linear, exponential, or a more abrupt decay, can be

observed depending on the different physical systems and conditions. This paper aimed to contribute to clarify how some different types of friction forces influence those shapes.

First, we will summarize the characteristics of the friction forces. The force of friction, of which the direction is always opposed to velocity, was applied along the surface of the contact of two bodies, impeding their relative motion. A distinction is usually made between dry (external) and viscous (internal) friction. Dry friction is the interaction between the surfaces of the two bodies. Viscosity is the interaction between layers of a fluid that are moving with respect to one another.

The dry friction considered is constant and occurs as the result of the plastic deformation of the two bodies. We designate it by $F_{Const} = \mu_{Theo} mg$, with μ_{Theo} the dimensionless kinetic friction coefficient.

The internal viscous forces must be separated into two components: pressure resistance, or drag, and friction drag. The resistance force is determined by the pressure difference at the front and rear edges of a body in a steam of fluid.

It depends on the density of the fluid, the square of the velocity, and the effective cross-section. We designate it by $F_{Quad} = \beta_{Theo} v^2$, with $\beta_{Theo} = C_b \frac{A_b}{2} \rho (\mathrm{kg/m})$ as the quadratic coefficient. The factor C_b mostly depends on the shape of the body, with typical values $C_b = 1.1$ for a round disk, $C_b = 0.4$ for a sphere, and $C_b = 0.004$ for a drop-shaped body.

The friction drag is determined by the forces of internal friction due to the large velocity gradient in the boundary layer. It depends on the viscosity, the velocity, and the size of the body. We designate it by $F_{Visc} = \lambda_{Theo} v$, where $\lambda_{Theo} = D_b \eta S_b (\mathrm{kg/s})$ is the viscous coefficient. Factor D_b is dimensionless (e.g., $D_b = 6\pi$ for a sphere), η is the coefficient of internal friction or viscosity of the fluid, and S_b is a characteristic dimension of the body.

At very low velocities, friction drag, which is proportional to the first power of the velocity, will be considerably greater than pressure drag, which is proportional to the square of the velocity. At higher velocities, the opposite will be true. To clarify the limits of low and high velocities, they are defined according to the global criterion, i.e., the Reynolds number, indicating the ratio of the pressure drag to the friction drag: $R_e = \frac{F_{rd}}{F_{fd}} \cong \frac{S_b \rho v}{\eta}$, extensively used in hydro- and aerodynamics. When $R_e < 1$, the pressure drag can be neglected, and only the friction drag is considered. For higher values of Reynolds numbers, only the pressure drag is considered, with the friction drag being neglected. The coexistence of these two forces is usually avoided.

Usually, in school textbooks, the only friction force considered acting on the mechanical oscillator is friction drag, proportional to velocity. This happens because, of the three types of friction, proportional to the first three powers of speed (0, 1, and 2), this is the only one with a mathematical expression that allows for a simple global didactic solution of the differential equation of movement. However, neglecting the constant dry friction has consequences in the description of the model. First, it has a natural important physical handicap, predicting a perpetual motion: the oscillations stop only after an infinite amount of time, and it is well known that the real physical oscillator stops after a relatively short time. Second, it is experimentally observed that the slope of the envelope line describing the decay of amplitude maxima, for small deformations, is linear instead of exponential. To overcome this difficulty, it is necessary to include more than one friction force.

In references [2–10], several authors approached this problem using different approximate technics, specially adding together the dry and viscous forces. This was also the case for references [3,9,11]. The constant force is addressed, for example, in references [4,7]. The quadratic force is addressed, for example, in references [8,10]. The three forces are separately discussed in reference [2]. Reference [1] provides the motivation for this phenomenological model used. References [5,6,12] provide the historical view of the scientific wealth existing in the use of the physical pendulum as a model. The models of nonlinear

oscillators and their behavior in the presence of friction forces do not fit the purpose of this manuscript. They can be followed by different authors (see, for example, references [13,14]).

In this paper, we discuss the contribution of the three friction force types, individually and together.

To obtain a consistent comparison, all the examples plotted have the same initial conditions: $t = 0 \Rightarrow x = x_0 = 1\text{ m} \wedge v = v_0 = 0$.

2. Notation

Let us consider the usual mechanical oscillator: a particle of mass m acted by an elastic force, of constant K, and a global dissipative force F_{Diss}, containing the three types of drag. For a deviation x from the equilibrium position, the oscillator motion ordinary differential equation ODE [1] is

$$m\frac{d^2x}{dt^2} = -Kx - F_{Diss} \quad \text{with} \quad F_{Diss} = \mu_T mg\frac{v}{|v|} + \lambda_T v + \beta_T v|v| \; ; \; v = \frac{dx}{dt} \tag{1}$$

The total energy is

$$E_T = \frac{1}{2}mv^2 + \frac{1}{2}Kx^2 \tag{2}$$

and the power equation is obtained multiplying Equation (1) by v:

$$\frac{dE_T}{dt} = -F_{Diss}\cdot v \tag{3}$$

For simplicity, let us consider that the motion of the particle starts at $x(0) = x_0$ with null velocity $v(0) = 0$. In order to obtain an equation independent of the physical characteristics of the oscillator and the initial position, we used the natural frequency $\omega_0 = \sqrt{\frac{K}{m}}$ and, instead of using time t and position x, we changed to two new variables: the relative deviation $r(t) = \frac{x(t)}{x_0}$ and a phase time $\tau = \omega_0 t$, in radians. New derivatives are now designed by $\dot{r} = \frac{dr}{d\tau}$ and Equation (1) becomes

$$\ddot{r} = -\dot{r} - \alpha_{Diss}, \quad \text{with} \quad \alpha_{Diss} = \frac{\mu_T g}{x_0\omega_0^2}\frac{\dot{r}}{|\dot{r}|} + \frac{\lambda_T}{m\omega_0}\dot{r} + \frac{\beta_T x_0}{m}\dot{r}|\dot{r}| \quad \text{and} \quad \dot{r} = \frac{d(x/x_0)}{d\tau} \tag{4}$$

The new dissipative acceleration allows us to designate new dimensionless parameters:

$$\mu = \frac{\mu_T g}{\omega_0^2 x_0}, \lambda = \frac{\lambda_T}{m\omega_0}, \beta = \frac{x_0\beta_T}{m}. \tag{5}$$

Function (2) for the total energy becomes

$$E_T = E_0\left(\dot{r}^2 + r^2\right) \text{ with the initial energy } E_0 = \frac{1}{2}Kx_0^2 \tag{6}$$

and the new equation for power is

$$\frac{d(E_T/E_0)}{d\tau} = -2\alpha_{Diss}\cdot\dot{r} = -2\mu|\dot{r}| - 2\lambda|\dot{r}|^2 - 2\beta|\dot{r}|^3. \tag{7}$$

Equation (4) is the ODE with the new normalized drag coefficients (5) that will be considered and solved numerically to obtain the extrema of both deviation and velocity. Simultaneously, using relation (6), energy evolution is evaluated. The method used was the fourth order Runge–Kutta with initial conditions $r(0) = 1$ and $\dot{r}(0) = 0$.

The solver software needed was built using the LabVIEW 2019 [15] platform, but any other ODE solver containing peak and valley detectors can be used. The fitting software and

plots were performed with ORIGIN 7.0 [16] program, but also, other equivalent programs can be used.

3. Phenomenological Model

The aim of this study was to obtain an envelope-modulating function for the oscillator amplitude, and its correlation to the friction coefficients. Assuming that the oscillator is harmonic, we look for a solution given by the product of the modulating function and a sinusoidal harmonic part. The simpler model possible is $r(\tau) = R(\tau)\cos(\varepsilon\tau)$, with $\varepsilon = \frac{\omega}{\omega_0}$. This emphasizes the modulating functions $\pm R(\tau)$, but has a handicap: it does not touch the extrema of $r(\tau)$. These are obtained when $\dot{r}\ (\tau) = 0$, i.e., at the nulls of velocity. These nulls appear not when $\cos(\varepsilon\tau) = \pm 1$, but when $\mathrm{tg}(\varepsilon\tau) = \frac{\dot{R}(\tau)}{\varepsilon R(\tau)} \neq 0$.

On the other hand, we know that velocity vanishes, for a harmonic function, for every constant half period. This property allows for the use of the simpler model for velocity instead of the model on displacement. Therefore, the modulated harmonic function for velocity should be

$$\dot{r}(\tau) = -V(\tau)\sin(\varepsilon\tau) \tag{8}$$

The amplitude model we look for must satisfy Equation (4), and we assume that it can be built with the combination of two sinusoids:

$$r(\tau) = R_1(\tau)\cos(\varepsilon\tau) + R_2(\tau)\sin(\varepsilon\tau) \tag{9}$$

A simple derivative of this equation gives the velocity in terms of functions $R_1(\tau)$ and $R_2(\tau)$:

$$\dot{r}(\tau) = \left(\dot{R}_1 + \varepsilon R_2\right)\cos(\varepsilon\tau) + \left(-\varepsilon R_1 + \dot{R}_2\right)\sin(\varepsilon\tau) \tag{10}$$

Comparing Expressions (10) and (8), the relations between $R_1(\tau)$, $R_2(\tau)$ and $V(\tau)$ are

$$\dot{R}_1 + \varepsilon R_2 = 0 \text{ and } V(\tau) = \varepsilon R_1 - \dot{R}_2 \tag{11}$$

Notice that the first condition must be verified for all τ:

$$R_2(\tau) = -\frac{1}{\varepsilon}\dot{R}_1(\tau) \tag{12}$$

The nulls of the velocity mean that $\sin(\varepsilon\tau) = 0$ and imply that the ith extrema of amplitude are

$$r_{extrema}(\tau_i) = \pm R_1(\tau_i) \tag{13}$$

Functions $\pm R_1(\tau)$ are in fact the continuous functions passing through all the extrema of deviation. Knowing $R_1(\tau)$ and using relation (12), one can obtain $R_2(\tau)$ and build a general solution (9) for displacement.

Solutions for velocity can be obtained using the second condition of (11): $V(\tau) = \varepsilon R_1 - \dot{R}_2$. Notice that this function, $V(\tau)$, is a modulating function and does not pass through the extrema of velocity given by the nulls of acceleration, but only touches $\dot{r}(\tau)$. Notice that the extrema of velocity do not correspond to nulls of deviation. Nevertheless, due to the characteristics of Equation (4), we expect that the function connecting the velocity extrema to be the same type as the one for deviation. In fact, we should have $V_{extrema}(\tau_j) = R_1(\tau_j)$. Notice that these τ_j correspond to the extrema of velocity, and are therefore different from the τ_i that correspond to the extrema of displacement.

4. Energy Calculations

Both energy and amplitude studies can be performed simultaneously. Defining the total normalized energy as $E_N(\tau) = \frac{E(\tau)}{E_0}$, we rewrite Equations (6) and (7) as follows:

$$E_N = \dot{r}^2 + r^2 \tag{14}$$

$$\frac{dE_N}{d\tau} = -2\mu|\dot{r}| - 2\lambda|\dot{r}|^2 - 2\beta|\dot{r}|^3 \tag{15}$$

By numerically solving Equation (4), we can also compute the normalized energy function from Equation (15).

Notice that if we consider the instants of displacement extrema, the energy is only due to the elastic force, and it is expected for the normalized energy function at these instants to be equal to the square of amplitude:

$$E_N^{extrema}(\tau) = R_1^2(\tau) \tag{16}$$

This simple property allows for a way to anticipate the mathematical structure of the extremum function $R_1(\tau)$. Using Equation (16) to describe the global behavior of energy, we obtain a new way to write the energy loss:

$$\frac{dE_N(\tau)}{d\tau} \cong \frac{dE_N^{extrema}(\tau)}{d\tau} = 2R_1(\tau)\frac{dR_1}{d\tau} \tag{17}$$

This expression follows the extremum line and neglects the details of energy variation inside each half period.

To obtain the same result, but using Equation (15), it is necessary to integrate over half a period:

$$\frac{dE_N(\tau)}{d\tau} \simeq \frac{\Delta E_N(\tau)}{\pi/\varepsilon} = -\frac{2\varepsilon}{\pi}\int_{\tau}^{\tau+\pi/\varepsilon}\left(\mu|\dot{r}| + \lambda|\dot{r}|^2 + \beta|\dot{r}|^3\right)d\tau \tag{18}$$

4.1. Integral Calculation Using the Velocity Extrema

To solve implicitly the integral in (18), we must ignore the amplitude variation during the half period of integration and consider only the sinusoidal variation associated with the dissipative force. Instead of the local form $V(\tau) = \varepsilon R_1 - \dot{R}_2$, it is necessary to use a constant amplitude within the half period. The appropriate form should be the corresponding extrema that we already know: $V_{extrema}(\tau) = R_1(\tau)$.

$$\begin{aligned}
&\int_{\tau}^{\tau+\pi/\varepsilon}\left(\mu|\dot{r}| + \lambda|\dot{r}|^2 + \beta|\dot{r}|^3\right)d\tau = \frac{1}{\varepsilon}\int_0^{\pi}\left(\mu R_1(\tau)\sin(\theta) + \lambda R_1^2(\tau)\sin^2(\theta) + \beta R_1^3(\tau)\sin^3(\theta)\right)d\theta = \\
&\simeq \frac{\mu}{\varepsilon}R_1(\tau)\int_0^{\pi}\sin(\theta)d\theta + \frac{\lambda}{\varepsilon}R_1^2(\tau)\int_0^{\pi}\sin^2(\theta)d\theta + \frac{\beta}{\varepsilon}R_1^3(\tau)\int_0^{\pi}\sin^3(\theta)d\theta = \\
&= \frac{2\mu}{\varepsilon}R_1(\tau) + \frac{\pi}{2}\frac{\lambda}{\varepsilon}R_1^2(\tau) + \frac{4}{3}\frac{\beta}{\varepsilon}R_1^3(\tau)
\end{aligned} \tag{19}$$

Using this result in Equations (17) and (18), we obtain an equation for function $R_1(\tau)$:

$$\frac{dR_1}{d\tau} = -\frac{2}{\pi}\mu - \frac{1}{2}\lambda R_1 - \frac{4}{3\pi}\beta R_1^2 \tag{20}$$

This is the fundamental equation needed to extract the extrema tail. We will use three new constant parameters, A, B, and C, to characterize the second order polynomial of

Equation (20). They are univocally related to each one of the coefficients, and allow for a clearer identification of the polynomial roots:

$$\frac{dR_1}{d\tau} = -\left(AR_1^2 + BR_1 + C\right) \Leftarrow \left(C = \frac{2\mu}{\pi} \quad B = \frac{\lambda}{2} \quad A = \frac{4\beta}{3\pi}\right)$$

4.2. Integral Calculation Using the Mean Velocity of the Undamped Oscillator

The result obtained in Section 4.1 can be achieved by using a different approach: the mean velocity of the undamped oscillator during each half period must be like the damped situation and, therefore, the first order differential equation for velocity is:

$$\dot{r}^2 + r^2 = R_1^2$$

R_1 stands for both amplitude and velocity extrema. A simple equation for velocity is obtained, and its mean values can be calculated as follows:

$$|\dot{r}| = \sqrt{R_1^2 - r^2} \Rightarrow \left|\bar{\dot{r}}\right| = \frac{1}{\pi}\int_0^{\pi} |\dot{r}| d\tau = \frac{2R_1}{\pi}$$

We also need the mean values of the square and the cube of velocity:

$$\left|\bar{\dot{r}}\right|^2 = \frac{1}{\pi}\int_0^{\pi} |\dot{r}|^2 d\tau = \frac{1}{\pi}\int_{-R_1}^{+R_1} |\dot{r}| dr = \frac{1}{\pi}\int_{-R_1}^{+R_1} \sqrt{R_1^2 - r^2} dr = \frac{R_1^2}{2};$$

$$\left|\bar{\dot{r}}\right|^3 = \frac{1}{\pi}\int_0^{\pi} |\dot{r}|^3 d\tau = \frac{1}{\pi}\int_{-R_1}^{+R_1} |\dot{r}|^2 dr = \frac{1}{\pi}\int_{-R_1}^{+R_1} \left(R_1^2 - r^2\right) dr = \frac{4R_1^3}{3\pi}$$

The three results are identical to those obtained in Section 4.1.

In the next sections, we will solve Equation (20) for several physical situations corresponding to different combinations of acting forces.

For every combination, we will use the same range for the three dimensionless parameters: $0.001 \leq \mu \leq 0.05$, $0.001 \leq \lambda \leq 0.5$, and $0.001 \leq \beta \leq 0.1$. These intervals have a correspondence to the real oscillator through Formula (5): $0.001 m\omega_0^2 \leq \mu_T \leq 0.05 m\omega_0^2$, $0.001 m\omega_0 \leq \lambda_T \leq 0.5 m\omega_0$, and $0.001 \frac{m}{x_0} \leq \beta_T \leq 0.1 \frac{m}{x_0}$.

5. Verification of the Exact Solution ($\mu = 0$, $\lambda \neq 0$, $\beta = 0$)

When only the viscous force is present, Equation (20), $\frac{dR_1}{d\tau} = -\frac{1}{2}\lambda R_1$, has a simple solution: $R_1(\tau) = e^{-\frac{\lambda}{2}\tau}$.

Using relation (11), the other term and the velocity can be evaluated: $R_2(\tau) = \frac{\lambda}{2\varepsilon} e^{-\frac{\lambda}{2}\tau}$ and $V(\tau) = \frac{1}{\varepsilon} e^{-\frac{\lambda}{2}\tau}$.

Converting to the usual coordinates (x,t), the known solutions are obtained:

$$\begin{cases} x = x_0 e^{-\frac{\lambda_T}{2m}t}\left(\cos(\omega t) + \frac{\lambda_T}{2m\omega}\sin(\omega t)\right) \\ v = -\frac{\omega_0^2}{\omega} x_0 e^{-\frac{\lambda_T}{2m}t}\sin(\omega t) \end{cases},$$

verifying the model.

6. Application to an Oscillator with Coulomb and Viscous Forces ($\mu \neq 0, \lambda \neq 0, \beta = 0$)

This is a natural extension of the previous case. The presence of the constant Coulomb force stops the oscillation naturally.

Equation (20) for this case takes the form $\frac{dR_1}{d\tau} = -(BR_1 + C)$, and its solution is $R_1(\tau) = \left(1 + \frac{C}{B}\right)e^{-B\tau} - \frac{C}{B}$.

The mathematical model necessary to adjust the oscillator data requires two parameters, P_1 and P_2:

$$R_1(\tau) = (1 + P_2)e^{-P_1\tau} - P_2$$

After the fit, the friction coefficients are $\mu = \frac{\pi}{2}P_1P_2$ and $\lambda = 2P_1$. The function obtained is

$$R_1(\tau) = \left(1 + \frac{4\mu}{\pi\lambda}\right)e^{-\frac{\lambda}{2}\tau} - \frac{4\mu}{\pi\lambda} \tag{21}$$

This function must be always positive and, therefore, the movement ends when $\tau_{final} = \frac{2}{\lambda}\ln\left(1 + \frac{\pi\lambda}{4\mu}\right)$. The oscillator stops after $n = \text{int}\left[\frac{\varepsilon}{\pi\lambda}\ln\left(1 + \frac{\pi\lambda}{4\mu}\right)\right]$ oscillations, because the system does not have enough energy to cross the Coulomb barrier threshold. Notice that this barrier corresponds to the slope of $R_1(\tau_{final})$. This slope, $\left(\frac{dR_1}{d\tau}\right)_{\tau_{final}} = -\frac{2\mu}{\pi}$, is proportional to the force coefficient.

The constant $\varepsilon = \frac{\omega}{\omega_0}$ can be evaluated by measuring the period from the several parameters sets and was verified to satisfy $\varepsilon = \sqrt{1 - \left(\frac{\lambda}{2}\right)^2}$.

Figures 1 and 2 show the results of function $R_1(\tau)$ and the numerical solution of Equation (4) for several combinations of parameters (μ, λ). The model adjusts very well in all tested cases, and numerical data are indistinguishable from model in both figures. To estimate the error, we compute the relative error $(r_{ext} - R_1)/r_{ext}$ for the case $\lambda = 0.1$ and $\mu = 0.005$, which is plotted in Figure 3. This error is less than 0.003%.

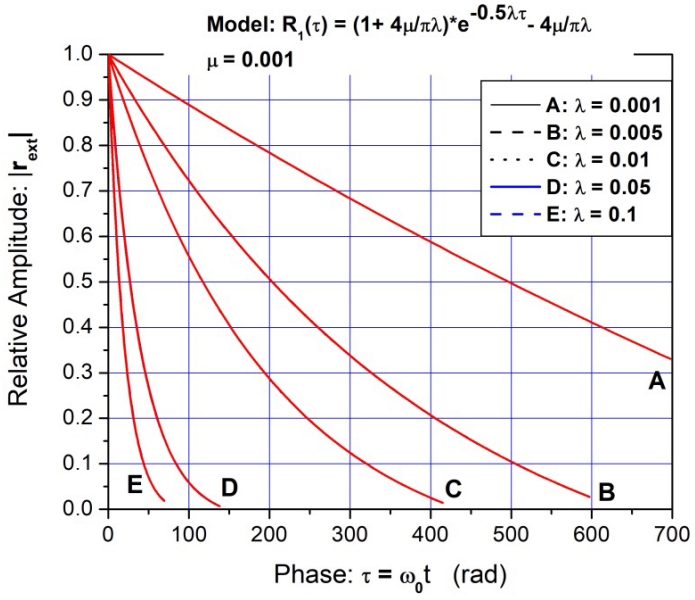


Figure 1. Deviation extremum modulus for several values of λ, with $\beta = 0$ and $\mu = 0.001$. The model used adjusts all cases very well, and the numerical data are indistinguishable from the model.

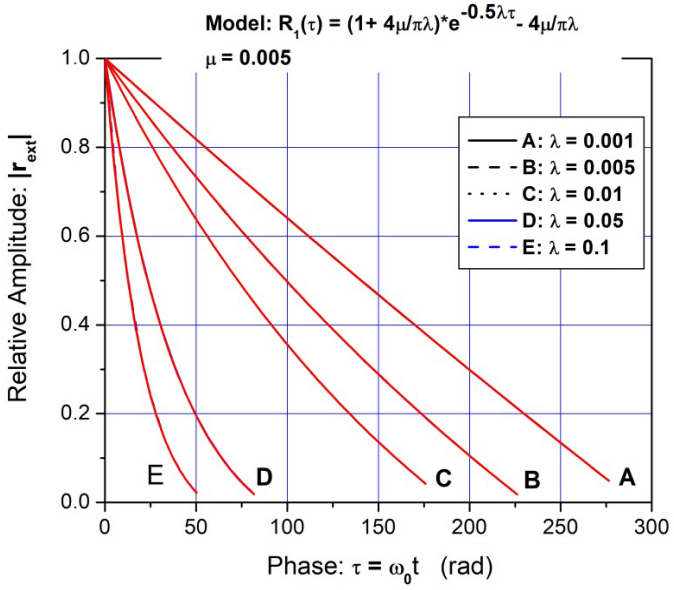


Figure 2. Deviation extremum modulus for several values of λ, with $\beta = 0$ and $\mu = 0.005$. The model used adjusts all cases very well, and the numerical data are indistinguishable from the model.

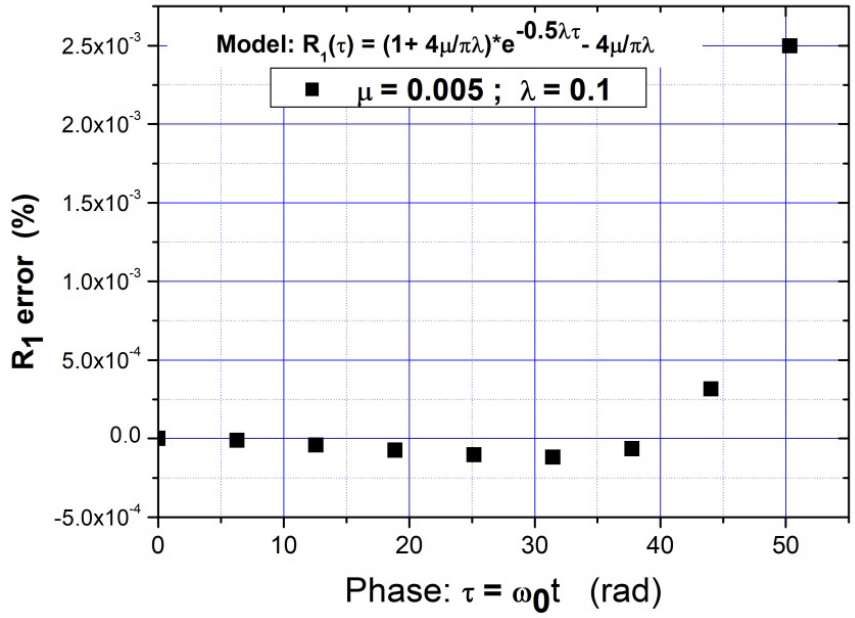


Figure 3. The evaluated error of R_1 model, in percentage, for the largest parameters of Figure 2 ($\lambda = 0.1$ and $\mu = 0.005$). The error is always less than 0.003%.

Using expression (12), we obtain $R_2(\tau)$:

$$R_2(\tau) = \frac{\lambda}{2\varepsilon} R_1(\tau) + \frac{2\mu}{\pi\varepsilon} = \frac{\lambda}{2\varepsilon}\left(1 + \frac{4\mu}{\pi\lambda}\right) e^{-\frac{\lambda}{2}\tau}, \tag{22}$$

and the general solution for displacement becomes

$$r(\tau) = \left[\left(1 + \frac{4\mu}{\pi\lambda}\right) e^{-\frac{\lambda}{2}\tau} - \frac{4\mu}{\pi\lambda}\right] \cos(\varepsilon\tau) + \left[\frac{\lambda}{2\varepsilon}\left(1 + \frac{4\mu}{\pi\lambda}\right) e^{-\frac{\lambda}{2}\tau}\right] \sin(\varepsilon\tau) \tag{23}$$

We verify that the velocity extrema modulus lay on the same function $R_1(\tau)$, but we are interested on the velocity envelope, given by function $V(\tau)$, that can be evaluated directly using Expression (8):

$$V(\tau) = \varepsilon R_1(\tau) - \dot{R}_2(\tau) = \frac{1}{\varepsilon}\left(1 + \frac{4\mu}{\pi\lambda}\right)e^{-\frac{\lambda}{2}\tau} - \frac{4\mu\varepsilon}{\pi\lambda} \tag{24}$$

Therefore, the general solution for velocity can be written as

$$\dot{r}(\tau) = \left[-\frac{1}{\varepsilon}\left(1 + \frac{4\mu}{\pi\lambda}\right)e^{-\frac{\lambda}{2}\tau} + \frac{4\mu\varepsilon}{\pi\lambda}\right]\sin(\varepsilon\tau) \tag{25}$$

The normalized energy function decreases after each cycle, following the amplitude square damping at the extrema, as expected. Figure 4 shows the $E_N(\tau)$ function, along with the $r(\tau)$ and $\dot{r}(\tau)$ extrema.

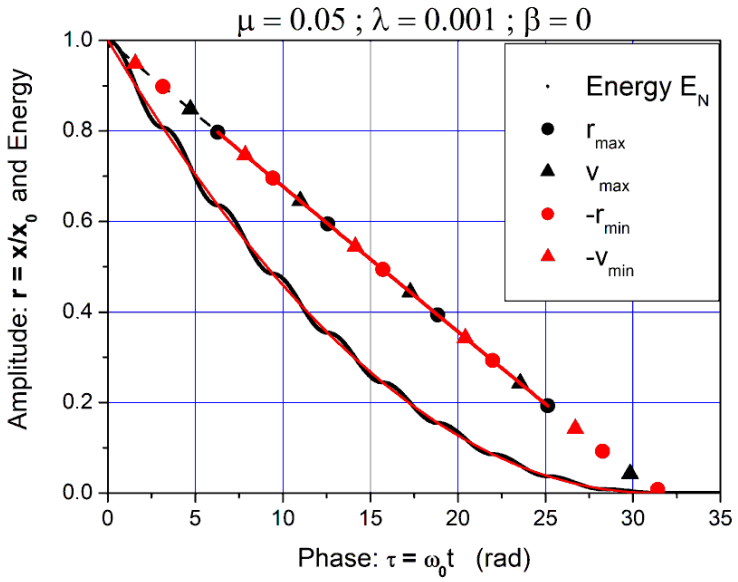


Figure 4. The energy $E_N(\tau)$ function. The extrema of the amplitude and the velocity are plotted. The line connecting the extrema corresponds to $R_1(\tau)$, i.e., Equation (20). The thin line crossing the $E_N(\tau)$ function corresponds to $R_1^2(\tau)$.

7. Oscillator with Only the Quadratic Turbulent Force ($\mu = 0, \lambda = 0, \beta \neq 0$)

In this case, the ODE (4) contains only one dissipative term:

$$\ddot{r} = -r - \beta\dot{r}|\dot{r}| \tag{26}$$

We separated this case because there is no analytical solution and, as we will see, the predicted mathematical expression for the envelope differs from the usual exponential model. The period for this case must also be studied.

- **The envelope when the quadratic turbulent force is present**

Equation (20) takes the form $\frac{dR_1}{d\tau} = -AR_1^2$ and has the solution $R_1(\tau) = \frac{1}{1+A\tau}$.

The mathematical model necessary to adjust the oscillator data requires only one parameter, P_1:

$$R_1(\tau) = \frac{1}{1 + P_1\tau}$$

After the fit, the friction coefficient is $\beta = \frac{3\pi}{4}P_1$. The type of function obtained is hyperbolic:

$$R_1(\tau) = \frac{1}{1 + \frac{4\beta}{3\pi}\tau} \tag{27}$$

The solutions of ODE (26) for values $0.001 \leq \beta \leq 0.1$ are plotted in Figure 5. The agreement between the numeric data and function (27) is very good for the entire range of parameter β tested.

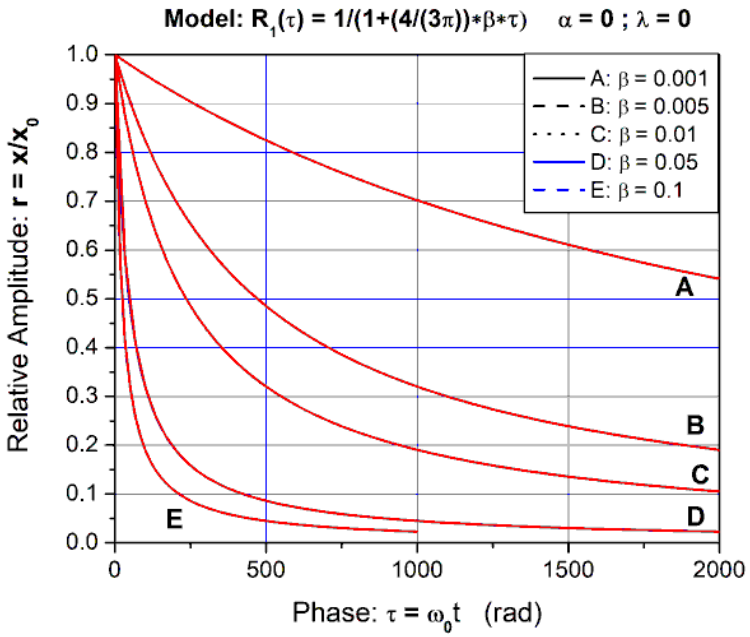


Figure 5. Oscillator with only turbulent friction. The adjusting model is hyperbolic, i.e., Equation (27), not exponential.

By using expression (12), we obtain $R_2(\tau)$:

$$R_2(\tau) = \frac{4}{3\pi\varepsilon}\beta R_1^2(\tau) = \frac{\frac{4}{3\pi\varepsilon}\beta}{\left(1 + \frac{4}{3\pi}\beta\tau\right)^2} \tag{28}$$

The general solution for displacement becomes

$$r(\tau) = \frac{1}{1 + \frac{4}{3\pi}\beta\tau}\cos(\varepsilon\tau) + \frac{\frac{4}{3\pi}\beta}{\left(1 + \frac{4}{3\pi}\beta\tau\right)^2}\sin(\varepsilon\tau) \tag{29}$$

Notice that the frequency ratio, represented by ε, can be a little smaller than unity for large β and amplitude values.

- **The period when the quadratic turbulent force is present**

Equation (26) can be transformed and integrated once to obtain the nulls of velocity and the half period.

For the first half period, with our initial conditions, we can write $\ddot{r} = -r + \beta\dot{r}^2$, because the velocity is negative.

Transforming acceleration into a space derivative, $\ddot{r} = \frac{1}{2}\frac{d\left(\dot{r}^2\right)}{dr}$, this equation takes the form $\frac{d\left(\dot{r}^2\right)}{dr} - 2\beta\dot{r}^2 = -2r$.

The two terms on the left side can be joined using the transformation $\frac{d\left(e^{-2\beta r}\dot{r}^2\right)}{dr} = e^{-2\beta r}\left(\frac{d\left(\dot{r}^2\right)}{dr} - 2\beta\dot{r}^2\right)$.

The resulting equation is $\frac{d\left(e^{-2\beta r}\dot{r}^2\right)}{dr} = -2re^{-2\beta r}$, that can be integrated:

$$\dot{r}^2 = -2e^{+2\beta r}\int_1^r re^{-2\beta r}dr$$

The integral on the right side can be performed, given $\int_1^r re^{-2\beta r}dr = \frac{1}{4\beta^2}\left[e^{-2\beta}(1+2\beta) - e^{-2\beta r}(1+2\beta r)\right]$.

Finally, we obtain the solution for velocity:

$$\dot{r} = -\frac{\sqrt{2}}{2\beta}\sqrt{1+2\beta r - Ae^{+2\beta r}} \quad \text{with} \quad A = \frac{1+2\beta}{e^{2\beta}}$$

Constant A is close to unity when parameter β is small but, for the highest value used, $\beta = 0.1$, $A = 0.9825$.

Besides $r = 1$, the other null of velocity, r_2, must be obtained from the transcendent equation $1 + 2\beta r = Ae^{+2\beta r}$.

This value corresponds to the first minimum of deviation and, inverting relation (27), we obtain the half period.

The usual way to obtain the first half period is to integrate the velocity equation (Table 1):

$$\tau = \int_1^r \frac{dr}{-\frac{\sqrt{2}}{2\beta}\sqrt{1+2\beta r - Ae^{+2\beta r}}} \Rightarrow \frac{T}{2} = \frac{2\beta}{\sqrt{2}}\int_{r_2}^1 \frac{dr}{\sqrt{1+2\beta r - Ae^{+2\beta r}}}$$

Table 1. This table presents the first minimum of deviation, evaluated using the Newton–Raphson method, and the first half period, using the R_1 model, for five values of parameter β.

β	First Minimum r_2	First Half Period
0.1	−0.882190	1.00157 × π
0.2	−0.788539	1.00563 × π
0.3	−0.711950	1.01148 × π
0.4	−0.647967	1.01867 × π
0.5	−0.593624	1.02685 × π

Numeric data for the period are also extracted from acceleration Equation (26) or velocity equation. In Figure 6, the results for the period are shown for several β values. It was verified that the movement is not always periodic: for smaller values of β, the oscillation keeps the natural period 2π but, for the largest values of β, the period starts from a value 0.13% higher and ends, after approximately 60 oscillations, with $\tau_0 = 2\pi$.

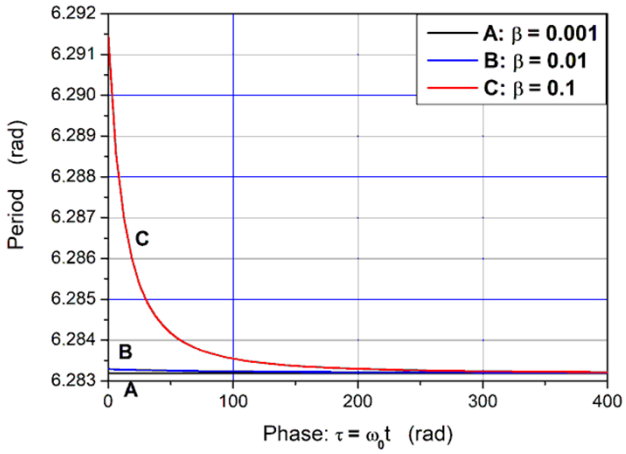


Figure 6. Period evolution of a system with turbulent force. For $\beta = 0.1$, the period starts at a value 0.13% higher, but rapidly approaches the natural value 2π. Notice that the whole phase scale presented, 400 rad, corresponds to 63 oscillations.

8. Oscillator with the Quadratic Plus Constant Dry Force ($\mu \neq 0, \lambda = 0, \beta \neq 0$)

Including the dry force to the last item, the ODE (4) has now two dissipative terms:

$$\ddot{r} = -r - \mu \frac{\dot{r}}{|\dot{r}|} - \beta \dot{r}|\dot{r}| \tag{30}$$

Equation (20) for this case ($\lambda = 0$) takes the form

$$\frac{dR_1}{d\tau} = -C - AR_1^2 \text{ with the solution: } R_1(\tau) = \frac{1 - \sqrt{\frac{C}{A}} tg\left(\tau\sqrt{AC}\right)}{1 + \sqrt{\frac{A}{C}} tg\left(\tau\sqrt{AC}\right)} \tag{31}$$

An alternative form can be used defining parameters θ_1 and θ_2:

$$tg\theta_1 = \sqrt{\frac{A}{C}} \text{ and } \theta_2 = \sqrt{AC} \Rightarrow R_1(\tau) = \frac{tg(\theta_1 - \theta_2\tau)}{tg(\theta_1)} \tag{32}$$

After the fit, the friction coefficients are $\mu = \frac{\pi}{2}\frac{\theta_2}{tg(\theta_1)}$; $\beta = \frac{3\pi}{4}\theta_2 tg(\theta_1)$.

The function obtained is a tangent type, and we notice that the movement ends when $\tau = \frac{\theta_1}{\theta_2}$.

Equation (30) was solved for $0.001 \leq \mu \leq 0.05$ and $0.001 \leq \beta \leq 0.1$. Some of the results are plotted in Figure 7, and very good agreement was achieved for all cases with the model deduced.

Using (12), we obtain the second function $R_2(\tau)$:

$$R_2(\tau) = -\frac{0.637\mu}{\cos^2(\theta_1 - \theta_2\tau)} \tag{33}$$

and the general solution for displacement:

$$r(\tau) = \frac{\text{tg}(\theta_1 - \theta_2\tau)}{\text{tg}(\theta_1)}\cos(\varepsilon\tau) - \frac{0.637\mu}{\cos^2(\theta_1 - \theta_2\tau)}\sin(\varepsilon\tau) \tag{34}$$

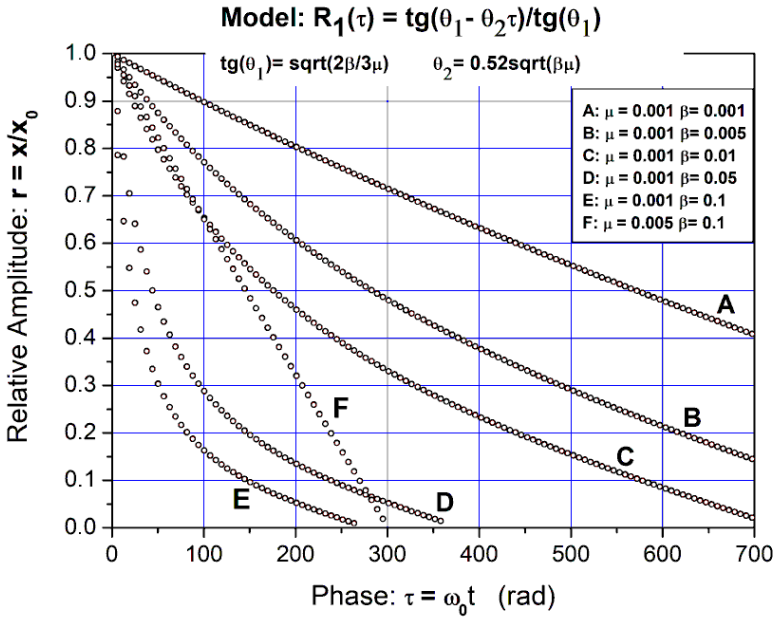


Figure 7. Oscillator with quadratic and constant friction. The adjusting model is a tangent-like function, i.e., Equation (32), and agreement is very good for all the tested cases.

9. Oscillator Containing Viscous and Quadratic Forces ($\mu = 0, \lambda \neq 0, \beta \neq 0$)

The ODE (4) has two dissipative terms:

$$\ddot{r} = -r - \lambda\dot{r} - \beta\dot{r}|\dot{r}| \tag{35}$$

Equation (20) for this case ($\mu = 0$) takes the form

$$\frac{dR_1}{d\tau} = -B - AR_1^2 \quad \text{with the solution:} \quad R_1(\tau) = \frac{e^{-B\tau}}{1 + \frac{A}{B}(1 - e^{-B\tau})} \tag{36}$$

The mathematical model necessary to adjust the oscillator data requires two parameters, P_1 and P_2:

$$R_1(\tau) = \frac{e^{-P_1\tau}}{1 + P_2(1 - e^{-P_1\tau})}$$

After the fit, the friction coefficients are $\beta = \frac{3\pi}{4}P_1P_2$ and $\lambda = 2P_1$.

Equation (35) was solved for $0.001 \leq \lambda \leq 0.1$ and $0.001 \leq \beta \leq 0.1$. Some of the results are shown in Figure 8.

By using Equation (12), we obtain $R_2(\tau)$:

$$R_2(\tau) = \frac{A + B}{\varepsilon}\frac{R_1(\tau)}{1 + \frac{A}{B}(1 - e^{-B\tau})}, \tag{37}$$

and the general solution for displacement:

$$r(\tau) = \frac{e^{-B\tau}}{1 + \frac{A}{B}(1 - e^{-B\tau})}\cos(\varepsilon\tau) + \frac{A + B}{\varepsilon}\frac{R_1(\tau)}{1 + \frac{A}{B}(1 - e^{-B\tau})}\sin(\varepsilon\tau) \tag{38}$$

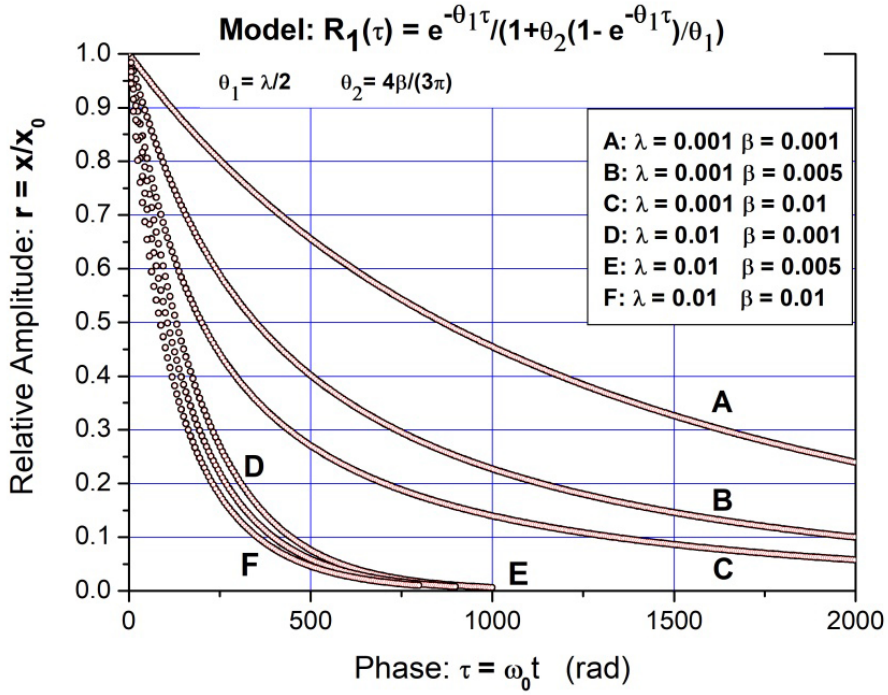


Figure 8. Oscillator with the viscous plus a quadratic friction force. The adjusting model is a combined exponential, Equation (35), and agreement with the numeric data is very good for all the tested cases.

10. Oscillator with the Three Friction Forces ($\mu \neq 0, \lambda \neq 0, \beta \neq 0$)

In this case, the ODE (4) does not simplify; all the terms must be included. Equation (20) for this general case predicts three types of solutions depending on the values of the parameters:

$$\frac{dR_1}{d\tau} = -\left(AR_1^2 + BR_1 + C\right) \tag{39}$$

The second-order polynomial may have real or complex roots, which leads to different types of mathematical solutions. We used three new constants, A, B, and C, to separate these roots, and the three different solution types are due to the discriminant signal: B^2 greater, less or equal to $4AC$.

Defining new constants, $K_1 = \frac{B}{2A} = \frac{3\pi\lambda}{16\beta}$ and $K_2 = \frac{C}{A} = \frac{3\mu}{2\beta}$, we must separate the three conditions.

For simplicity, the approximate constant $\frac{8}{\pi}\sqrt{\frac{2}{3}} \simeq 2.08$ is used.

10.1. The Frontier Case: $B^2 = 4AC \Rightarrow \lambda = 2.08\sqrt{\mu\beta}$

There exists a special solution for Equation (38) when $B^2 = 4AC$:

$$K_1^2 = K_2 \Leftrightarrow \lambda = 2.08\sqrt{\mu\beta} \Rightarrow R_1(\tau) = \frac{1 - \frac{B}{2}\left(1+\sqrt{C}\right)\tau}{1 + A\left(1+\sqrt{C}\right)\tau} \tag{40}$$

Using (12), we obtain $R_2(\tau)$: $R_2(\tau) = \frac{\left(1+\sqrt{C}\right)\left(A+\sqrt{AC}\right)}{\varepsilon\left(1+A\left(1+\sqrt{C}\right)\tau\right)^2}$.

10.2. When the Viscous Force Is Dominant: $\lambda > 2.08\sqrt{\mu\beta}$

The solution for Equation (39) when $B^2 > 4AC$ is mathematically of the exponential type:

$$K_1^2 > K_2 \Leftrightarrow \lambda > 2.08\sqrt{\mu\beta}; \Delta = \sqrt{B^2 - 4AC}\,; K = \frac{2A + B - \Delta}{2A + B + \Delta} \Rightarrow R_1(\tau) = \frac{1}{2A}\left(-B + \Delta\frac{1 + Ke^{-\Delta\tau}}{1 - Ke^{-\Delta\tau}}\right) \tag{41}$$

To adjust the oscillator data, one needs four parameters, with three being linearly independent. We used $\left[P_1 = K_1, P_2 = \sqrt{K_1^2 - K_2}, P_3 = \Delta, P_4 = K = \frac{1+P_1-P_2}{1+P_1+P_2}\right]$:

$$R_1(\tau) = -P_1 + P_2\frac{1 + P_4e^{-P_3\tau}}{1 - P_4e^{-P_3\tau}}$$

After the fit, the friction coefficients are $\mu = \frac{\pi}{4}\frac{P_3}{P_2}\left(P_1^2 - P_2^2\right)$, $\lambda = 2\frac{P_1P_3}{P_2}$, $\beta = \frac{3\pi}{8}\frac{P_3}{P_2}$. Using (12), we obtain the second function: $R_2(\tau) = \frac{K\Delta^2e^{-\Delta\tau}}{\varepsilon A\left(1-Ke^{-\Delta\tau}\right)^2}$.

10.3. When the Turbulent or Constant Forces Together Are Dominant: $\lambda < 2.08\sqrt{\mu\beta}$

The solution for Equation (39), when $B^2 < 4AC$, is of the tangent type:

$$K_1^2 < K_2 \Leftrightarrow \lambda < 2.08\sqrt{\mu\beta}; \Delta = \sqrt{4AC - \mathrm{B}^2}\ ;\ \mathrm{tg}\theta_0 = \frac{2A+B}{\Delta} \Rightarrow R_1(\tau) = \frac{1}{2A}\left(-B + \Delta\mathrm{tg}\left(\theta_0 - \frac{\Delta}{2}\tau\right)\right) \quad (42)$$

To adjust the oscillator, data are needed for the four parameters: three independent plus one dependent.

We used $\left[P_1 = K_1, P_2 = \sqrt{K_1^2 - K_2}, P_3 = \Delta, P_4 = \theta_0 = arc\mathrm{tg}\left(\frac{1+P_1}{P_2}\right)\right]$:

$$R_1(\tau) = -P_1 + P_2\mathrm{tg}\left(P_4 - \frac{P_3}{2}\tau\right)$$

After the fit, the friction coefficients are, as before, $\mu = \frac{\pi}{4}\frac{P_3}{P_2}\left(P_1^2 - P_2^2\right)$, $\lambda = 2\frac{P_1P_3}{P_2}$, $\beta = \frac{3\pi}{8}\frac{P_3}{P_2}$.

Using (12), we obtain the second function: $R_2(\tau) = \frac{\Delta^2}{4\varepsilon A\cos^2\left(\theta_0 - \frac{\Delta}{2}\tau\right)}$.

Equation (4) was solved for $0.001 \le \mu \le 0.1$, $0.001 \le \lambda \le 0.1$, and $0.001 \le \beta \le 0.1$. Some of the examples satisfy model (41) and the others satisfy model (42). We chose six examples of each type and plotted it in Figure 9 (model 42) and Figure 10 (model 41). All the examples show very good agreement between the models and the calculated extrema.

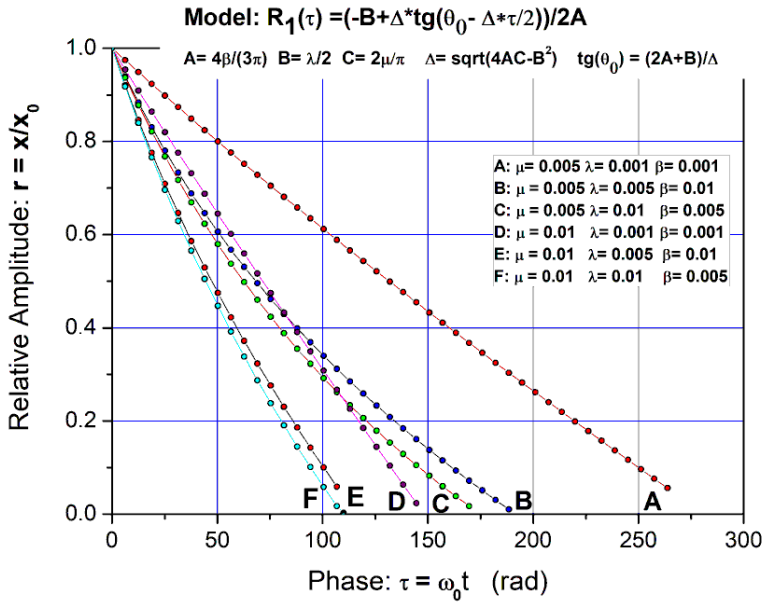


Figure 9. Oscillator in the presence for the three friction forces. The coefficients used in these six examples correspond to the case $\lambda < 2.08$*sqrt ($\mu\beta$). The adjusting model is a tangent; agreement is very good for all the tested examples.

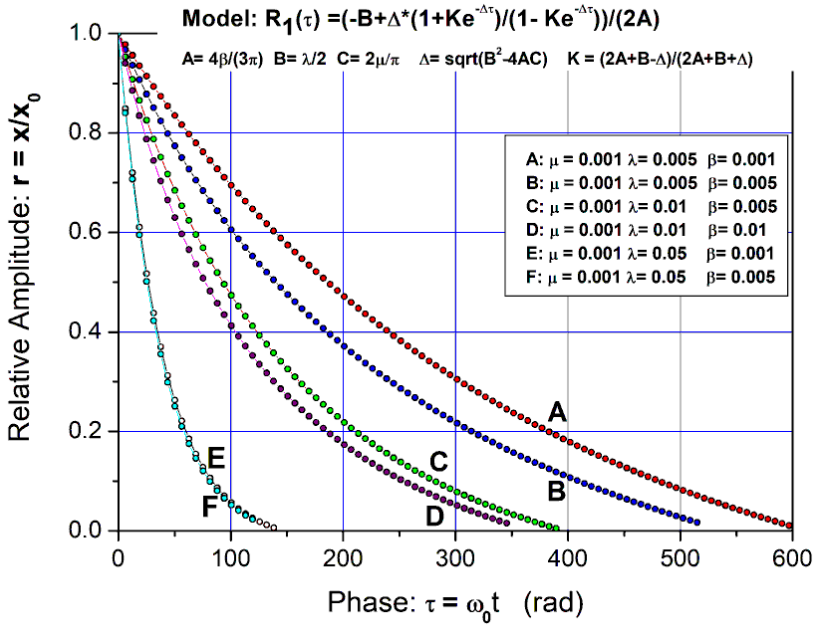


Figure 10. Oscillator in the presence of the three friction forces. The coefficients used in the six examples shown correspond to $\lambda > 2.08$*sqrt ($\mu\beta$). The adjusting model is exponential; agreement is very good for all the tested cases.

11. Conclusions

This work shows that the linear oscillator containing the usual three damping forces can be suitably characterized using a phenomenological model based on the extremum amplitude function.

We used a generic mechanical oscillator of mass m and elastic constant K, with initial conditions $x(0) = x_0$ and velocity $v(0) = 0$. The natural frequency was $\omega_0 = \sqrt{\frac{K}{m}}$, and was assumed to be the presence of three types of friction forces:

1. Constant dry friction: $-\mu_R \frac{v}{|v|}$, latter characterized by constant $\mu = \frac{\mu_R}{Kx_0}$;
2. Viscous drag: $-\lambda_R v$, latter characterized by constant $\lambda = \frac{\lambda_R}{m\omega_0}$;
3. Turbulent drag: $-\beta_R v|v|$, latter characterized by constant $\beta = \frac{x_0\beta_R}{m}$.

The index R was used to designate the force coefficients $(\mu_R, \lambda_R, \beta_R)$, while the non-indexed designated acceleration coefficients (μ, λ, β).

Five different physical situations were considered and solved. For each case, a convenient extremum function was found:

1. Quadratic force neglected

The mathematical model necessary to adjust the oscillator data requires two parameters, P_1 and P_2:

$$R_1(\tau) = (1 + P_2)e^{-P_1\tau} - P_2$$

After the fitting process, the friction coefficients obtained are $\mu = \frac{\pi}{2}P_1P_2$ and $\lambda = 2P_1$.

2. Quadratic force only

The mathematical model necessary to adjust the oscillator data requires one parameter, P_1:

$$R_1(\tau) = \frac{1}{1 + P_1\tau}$$

After the fitting process, the friction coefficient obtained is $\beta = \frac{3\pi}{4}P_1$.

3. Viscous force neglected

The mathematical model necessary to adjust the oscillator data needs two parameters, θ_1 and θ_2:

$$R_1(\tau) = \frac{\mathrm{tg}(\theta_1 - \theta_2\tau)}{\mathrm{tg}(\theta_1)}$$

After the fitting process, the friction coefficients obtained are $\mu = \frac{\pi}{2}\frac{\theta_2}{\mathrm{tg}(\theta_1)}$; $\beta = \frac{3\pi}{4}\theta_2\mathrm{tg}(\theta_1)$.

4. Constant force neglected

The mathematical model necessary to adjust the oscillator data requires two parameters, P_1 and P_2:

$$R_1(\tau) = \frac{e^{-P_1\tau}}{1 + P_2(1 - e^{-P_1\tau})}$$

After the fitting process, the friction coefficients obtained are $\beta = \frac{3\pi}{4}P_1P_2$; $\lambda = 2P_1$.

5. Three friction forces present: $\left(A = \frac{4\beta}{3\pi}; B = \frac{\lambda}{2}; C = \frac{2\mu}{\pi}\right)$

   - The frontier case: $B^2 = 4AC \Rightarrow \lambda = 2.08\sqrt{\mu\beta}$

$$R_1(\tau) = \frac{1 - \frac{B}{2}\left(1 + \sqrt{C}\right)\tau}{1 + A\left(1 + \sqrt{C}\right)\tau}$$

   - When the viscous force is dominant, $\lambda > 2.08\sqrt{\mu\beta}$

$$R_1(\tau) = -P_1 + P_2\frac{1 + P_4e^{-P_3\tau}}{1 - P_4e^{-P_3\tau}}$$

   After the fitting process, the friction coefficients obtained are $\mu = \frac{\pi}{4}\frac{P_3}{P_2}\left(P_1^2 - P_2^2\right)$, $\lambda = 2\frac{P_1P_3}{P_2}$, $\beta = \frac{3\pi}{8}\frac{P_3}{P_2}$

   - When the turbulent or constant forces together are dominant, $\lambda < 2.08\sqrt{\mu\beta}$

$$R_1(\tau) = -P_1 + P_2\mathrm{tg}\left(P_4 - \frac{P_3}{2}\tau\right)$$

   After the fitting process, the friction coefficients obtained are, as before, $\mu = \frac{\pi}{4}\frac{P_3}{P_2}\left(P_1^2 - P_2^2\right)$, $\lambda = 2\frac{P_1P_3}{P_2}$, $\beta = \frac{3\pi}{8}\frac{P_3}{P_2}$.

Funding: This research received no external funding.

Data Availability Statement: The original contributions presented in this study are included in the article. Further inquiries can be directed to the corresponding author.

Conflicts of Interest: The author declares no conflicts of interest.

References

1. Fernandes, J.C.; Sebastião, P.J.; Gonçalves, L.N.; Ferraz, A. Study of large-angle anharmonic oscillations of a physical pendulum using an acceleration sensor. *Eur. J. Phys.* **2017**, *38*, 4. [CrossRef]
2. Wang, X.S.; Schmitt, C.; Payne, M. Oscillations with three damping effects. *Eur. J. Phys.* **2002**, *23*, 155–164. [CrossRef]
3. Hinrichsen, P.F.; Larnder, C.I. Combined viscous and dry friction damping of oscillatory motion. *Am. J. Phys.* **2018**, *86*, 577. [CrossRef]
4. Li, A.; Ma, L.; Keene, D.; Klingel, J.; Payne, M.; Wang, X.-J. Forced oscillations with linear and nonlinear damping. *Am. J. Phys.* **2016**, *84*, 32–37. [CrossRef]

5. Nelson, R.A.; Olsson, M.G. The pendulum-rich physics from a simple system. *Am. J. Phys.* **1986**, *54*, 112–121. [CrossRef]
6. Squire, P.T. Pendulum damping. *Am. J. Phys.* **1986**, *54*, 984–991. [CrossRef]
7. Vitorino, M.V.; Vieira, A.; Rodrigues, M.S. Effect of sliding friction in harmonic oscillators. *Sci. Rep.* **2017**, *7*, 3726–3731. [CrossRef] [PubMed]
8. Mungan, C.E.; Lipscombe, T.C. Oscillations of a quadratically damped pendulum. *Eur. J. Phys.* **2013**, *34*, 1243–1253. [CrossRef]
9. Liang, J.-W. Identifying Coulomb and viscous damping from free-vibration acceleration decrements. *J. Sound Vib.* **2005**, *282*, 1208–1220. [CrossRef]
10. Cveticanin, L. Oscillator with strong quadratic damping force. *Publ. L'Institute Math.* **2009**, *85*, 119–130. [CrossRef]
11. Karthik, B.K.; Shreesha, R.B.; Shrikanth, V.; Gaonkar, A.K. Prediction of energy dissipation by analytical solution to combined viscous and Coulomb damping. *J. Sound Vib.* **2024**, *573*, 118216. [CrossRef]
12. Rogalsky, M.S.; Palmer, S. *Advanced University Physics*; CRC Press: Boca Raton, FL, USA; Taylor & Francis: Oxford, UK, 2006.
13. Kovacic, I.; Brennan, M.J.; Waters, T.P. A study of a nonlinear vibration isolator with a quasi-zero stiffness characteristic. *J. Sound Vib.* **2008**, *315*, 700–711. [CrossRef]
14. Kovacic, I.; Brennan, M.J. *The Duffing Equation: Nonlinear Oscillators and Their Behavior*; John Wiley & Sons: Hoboken, NJ, USA, 2011.
15. LabVIEWTM is a Product from National Instruments. Available online: http://www.ni.com (accessed on 18 July 2025).
16. ORIGINTM is a Product from Origin Lab—Data Analysis and Graphical Software. Available online: http://www.originlab.com (accessed on 18 July 2025).

Disclaimer/Publisher's Note: The statements, opinions and data contained in all publications are solely those of the individual author(s) and contributor(s) and not of MDPI and/or the editor(s). MDPI and/or the editor(s) disclaim responsibility for any injury to people or property resulting from any ideas, methods, instructions or products referred to in the content.